2020 8th IEEE International Conference on Biomedical
Robotics and Biomechatronics (BioRob)
New York, USA. Nov 29 - Dec 1, 2020

Testing Simulated Assistance Strategies on a Hip-Knee-Ankle Exoskeleton: a Case Study

Patrick W. Franks*, *Student Member, IEEE*, Nicholas A. Bianco*, Gwendolyn M. Bryan, Jennifer L. Hicks, Scott L. Delp, Steven H. Collins, *Member, IEEE*

***Abstract*— While exoskeletons have markedly reduced the metabolic cost of walking, exoskeleton design remains expensive and time-consuming. Biomechanical simulations could improve exoskeleton development with their ability to optimize many design and control parameters simultaneously. While promising, simulations often rely on simplifying assumptions, such as fixed kinematic methods. Furthermore, few simulation-based designs have been tested directly in human experiments. To evaluate the utility of simulations for exoskeleton design, we designed a controller using biomechanical simulation and then tested the controller with a hip-knee-ankle exoskeleton worn by a single experienced user. Here we show that a biomechanical simulation constrained by safe, experiment-based torque limits can find an assistance pattern that reduces metabolic cost but with substantial differences between expected and measured outcomes. We found a simulated assistance profile that was expected to reduce the metabolic cost of walking by 69.0%. When tested experimentally, it reduced the cost by 25.9% compared to walking in the device unassisted. The simulation predicted the direction of activity change in most muscles but overestimated the total magnitude of these changes. The applied torques resulted in joint kinematic and stride frequency changes that were not accounted for in the simulation. Future simulations could allow kinematic adaptations and use updated cost functions that better reflect how humans respond to assistance. Continued feedback between experimental testing and simulation design will build on these promising results to improve the accuracy of simulations and enhance their ability to guide future exoskeleton designs.**

I. INTRODUCTION

Exoskeletons and other wearable robots have the potential to improve human mobility. In recent years, exoskeletons have demonstrated improvements to a variety of gait parameters [1]. One popular goal for wearable robots is to reduce the energy used during walking, typically referred to as metabolic cost [1].

Recently, human-in-the-loop optimization has emerged as a technique to improve the performance of exoskeletons. Instead of relying on biomimicry, intuition, and hand-tuning, this technique uses measurements of the exoskeleton user to update the control of the exoskeleton to minimize a cost function. This approach has led to some of the largest reductions in metabolic cost to date [2], [3].

While human-in-the-loop optimization can identify effective assistance patterns, experiment times are long. As devices become more complex, either more assumptions about assistance must be made or more controller parameters must be optimized, which could eliminate potentially effective strategies or lead to longer optimization times. Ensuring that a user is trained sufficiently to utilize each control strategy also increases the time required to perform experimental optimization. Not only are these experiments expensive, long experiments can be prohibitive for people with walking impairments.

Biomechanical simulations provide a potential method to speed up wearable robot development [4], [5]. These simulations use models of the musculoskeletal system to analyze gait beyond what is measured in experiments by estimating, for example, joint loading and muscle-level metabolic energy consumption. Simulations can optimize many more device parameters than are reasonable to test experimentally. Simulations can optimize for cost functions that are not easily measured, such as muscle forces. Simulation results can also be used as initial guesses for human-in-the-loop optimizations, which could reduce experiment times.

Recently, simulation has been used to study exoskeleton assistance for normal walking, loaded walking, running, sit-to-stand tasks, and pathological gait [6]. Torque profiles developed using musculoskeletal simulation [4] have inspired exosuit control that produced experimental reductions in metabolic cost [7]. Despite this successful example and increasingly available device simulations, few assistance strategies designed in simulation have been tested directly in experiments.

The limitations of current simulations may be hindering adoption. For example, simulation approaches that optimize assistance assume cost functions that may not accurately reflect the true cost function of the user, leading to discrepancies between simulated and experimental muscle coordination and metabolic results. In addition, simulation approaches based on inverse dynamics do not account for changes in user kinematics or kinetics with assistance. Finally, current computational models of metabolic energy have been validated on isolated experiments of mammalian muscle fibers, but have yet to be fully validated for predicting changes in

*These authors contributed equally to this work

P. W. Franks, N. A. Bianco, and G. M. Bryan are with the Department of Mechanical Engineering, Stanford University, Building 530, 440 Escondido Mall, Stanford, CA 94305, USA pfranks@stanford.edu, nbianco@stanford.edu, gbryan@stanford.edu

J. L. Hicks is with the Department of Bioengineering, Stanford University, 443 Via Ortega, Stanford, CA 94305, USA jenhicks@stanford.edu

S. L. Delp is with the faculty of the Department of Mechanical Engineering, Department of Bioengineering, and Department of Orthopaedic Surgery, Stanford University, Building 530, 440 Escondido Mall, Stanford, CA 94305, USA delp@stanford.edu

S. H. Collins is with the faculty of the Department of Mechanical Engineering, Stanford University, Building 530, 440 Escondido Mall, Stanford, CA 94305, USA stevecollins@stanford.edu

978-1-7281-5907-2/20/$31.00 ©2020 IEEE

whole-body metabolic energy with exoskeleton assistance.

To better understand the accuracy of simulated exoskeleton assistance, we designed a controller for hip-knee-ankle assistance in simulation and tested that controller on a person using an exoskeleton. We constrained the simulation to ensure the design's torques would be within magnitudes comfortable for an experienced user during walking. We had a user walk with the simulation-designed assistance for two hours of training over two days and measured the effectiveness of the assistance on a third day. We compared the kinematics, muscle activity, and metabolic costs of the user in the experiment to the predicted values from simulation. We also compared measured metabolic cost to walking with assistance previously found through human-in-the-loop optimization.

Designing assistance in simulation could improve the development of exoskeletons and other wearable robots. With this work we aim to identify how simulations can inform experiments and how experiments can inform simulations. These observations could improve simulations, speed device development, and produce better assistive technology.

II. SIMULATION METHODS

We used musculoskeletal simulation to design torque profiles to be delivered by our exoskeleton. Our musculoskeletal model had a single leg with three degrees-of-freedom in the sagittal plane (hip flexion-extension, knee flexion-extension, and ankle plantarflexion-dorsiflexion) and 9 lower-limb muscles that could produce the major functions of normal gait (Fig. 1A). The model's muscle parameters and geometry paths were based on a previous study [8].

We used 3 previously-collected gait cycles of motion capture data from 3 healthy male subjects (mean $\pm$ s.d.: 71.73 $\pm$ 9.35 kg) during treadmill walking at 1.25 m/s including marker trajectories, ground reaction forces, and electromyography (EMG) measurements [9]. These subjects were different from the exoskeleton user in our experiments. The generic model's segment dimensions, mass parameters, and muscle optimal fiber lengths were scaled based on measured masses and static marker trials for each subject using the OpenSim musculoskeletal modeling software package [10]. The scaled models were then used to compute joint angles, joint angular velocities, muscle-tendon lengths and velocities, and muscle moment arms for each gait cycle using OpenSim's Inverse Kinematics tool. The net joint moments computed from OpenSim's Inverse Dynamics were qualitatively similar to joint moments of typical unassisted walking (Fig. 2). Muscle maximum isometric force parameters were scaled for each subject based on a previously established correlation between subject mass and muscle volume [11]. Passive muscle force-length curves were calibrated to match experimental passive joint moment measurements [12].

We modified an existing direct collocation optimal control framework [13] to solve three different types of problems: EMG-driven muscle parameter calibration, unassisted muscle redundancy resolution, and assistive device optimization. In each problem, muscle activation and tendon compliance dynamics were enforced and muscle-generated moments were constrained to match the net joint moments computed from inverse dynamics. Each problem included reserve torque actuators in addition to muscle-generated moments to help ensure dynamic consistency; these actuators were penalized heavily in the objective function such that the muscles were the primary actuators enforcing the joint moment constraints.

One gait cycle was used for EMG-driven muscle parameter calibration where muscle optimal fiber lengths, tendon slack lengths, and passive muscle force parameters were adjusted (by no more than 25% of their original value) to minimize differences between muscle excitations and EMG data. An additional low-weighted cost term that minimized muscle activation was included to find a unique solution for muscles without EMG data (iliopsoas and biceps femoris short head) and to improve problem convergence. The scaled models for each subject were updated with the new parameter values to be used in the unassisted and assistive device simulations.

Unassisted and assisted gait were simulated each using the remaining two gait cycles for each subject. In both cases, the primary objective was to minimize metabolic cost computed from a modified version of the metabolic energy model developed by Umberger et al. [14] with a continuous first derivative designed for gradient-based optimization [15]. Additional secondary objective terms minimizing muscle excitation, activation, and the derivative of tendon force were included to aid problem convergence. Since our simulation method relied on kinematics obtained from an inverse kinematics solution, the unassisted and assisted simulations used the same healthy walking kinematics (i.e., the simulation did not change the model's kinematics in response to the assistive device). In the unassisted simulations, the muscles and the heavily-penalized reserve torque actuators were the only actuators available to reproduce the net joint moments. In the assisted simulations, massless torque actuators with no power limits were added to the problem to help enforce the net joint moment constraint while reducing muscle effort. These actuators provided torque in hip flexion-extension, knee flexion-extension, and ankle plantarflexion to mimic the topology of our exoskeleton system. Ankle dorsiflexion was not assisted in simulation since our exoskeleton does not apply torque to this degree of freedom. We did not add mass to the leg segments or impedance to the joints of the model to represent the mass and passive impedance of the exoskeleton. However, mass and stiffness effects would be the same in assisted and unassisted conditions, which may cause an offset in metabolic cost but would not substantially change the difference in metabolic cost between conditions.

We solved the assisted problem using torque magnitude limits based on what was found to be reasonably comfortable during previous experiments: 0.5 N·m/kg for hip extension-flexion, 0.15 N·m/kg for knee extension-flexion, and 0.8 N·m/kg for ankle plantarflexion. These torque magnitude limits were imposed after initial simulations found assistance torques that were too large to safely test on a participant. We did not limit the shape of the torque profiles from applying

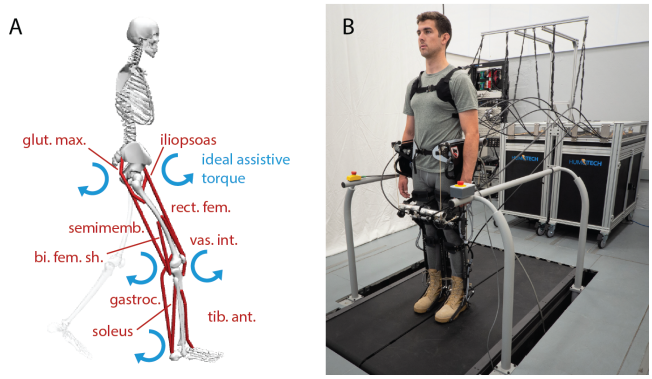

Fig. 1. **Simulated and experimental exoskeleton assistance.** (**A**) The musculoskeletal model used to design assistance in simulation included 9 primary sagittal-plane, lower-limb muscles and ideal torques in hip flexion-extension, knee flexion-extension, and ankle plantarflexion. (**B**) The designed assistance was tested using a bilateral hip-knee-ankle exoskeleton. The exoskeleton uses powerful off-board motors behind the treadmill to actuate a worn end effector using Bowden cable transmissions.

antagonist exoskeleton assistance (e.g., device hip flexion torque during biological hip extension torque). The device torque profiles were not parameterized and were free to take any shape allowed by the optimization problem, resulting in profiles that were more complex than the profiles that can be currently optimized in human-in-the-loop experiments. The simulation-optimized torque profiles were not constrained to be periodic across the gait cycle.

Metabolic cost was computed for both unassisted and assisted simulations by doubling the integrated metabolic rate summed across all muscles (assuming mediolateral symmetry), dividing by the gait cycle duration and whole body mass. The unassisted optimizations produced muscle activity that was qualitatively similar to the EMG recordings for each subject. The metabolic cost of walking computed by the metabolics model was 1.96 $\pm$ 0.25 W/kg across subjects. This cost does not include a basal metabolic rate. We computed percent differences in metabolic cost between unassisted and assisted conditions to assess the effects of assistance on the energy cost of walking.

III. Experimental Methodology

We tested the simulation-designed torque profile on a hip-knee-ankle exoskeleton. The simulated assistance profile was tested on a single experienced user (male, 186 cm, 90 kg) walking on a treadmill at 1.25 m/s. This user had walked in the exoskeleton with applied torques for over 50 hours in the past year, including human-in-the-loop optimization of hip-knee-ankle assistance. We conducted the test on an experienced user and used a training protocol to reduce possible effects of training so that the simulated assistance had the best chance to be successful. The participant provided written informed consent before participation, after the nature and possible consequences of the study were explained. The study protocol was approved and overseen by the Institutional Review Board of Stanford University and the US Army Medical Research and Materiel Command (USAMRMC) Office of Research Protections.

A. Exoskeleton Hardware and Control

Experimental evaluation of the simulated assistance was conducted using a hip-knee-ankle exoskeleton [16] (Fig. 1B). This system uses powerful off-board motors located behind the user who walks on a treadmill. The offboard motors apply torques using a Bowden cable transmission. The exoskeleton has a worn mass of 13.5 kg. The exoskeleton's carbon fiber struts are compliant in unactuated directions to minimize restriction of the user. The exoskeleton can apply 200 N·m in hip flexion and extension, 250 N·m in knee extension, 140 N·m in knee flexion, and 200 N·m in ankle plantarflexion. There is no dorsiflexion assistance. Applied torques are directly measured on the exoskeleton via load cells and strain gauges. When no torque is applied in a direction of actuation, the transmission is slack, allowing the user to move freely.

The exoskeleton applies torques as a function of percent stride, which is measured as the time since heel strike divided by average stride time. Heel strikes are registered using ground reaction force measurements from the treadmill. The torque profiles from simulation were prescribed as a function of percent stride and scaled by the user's body mass. Due to knee extension safety and hardware limitations, knee extension torque was constrained when the knee angle was small. To evaluate the effect of torque-tracking limitations of the exoskeleton hardware, we measured applied torque and compared to the desired torque to calculate root-mean-squared tracking error.

B. Training Protocol

The user went through a training protocol to ensure they could utilize the exoskeleton assistance fully. Training occurred over two consecutive days. Each day consisted of three bouts of 20 minutes of walking in applied torques. Five minute breaks were given between each of the 20 minute bouts of walking. Metabolic cost was measured throughout training.

C. Evaluation Protocol

After two training days, evaluation was conducted on a third day. Each condition was evaluated in two trials using a double-reversal framework ("ABCD DCBA") to improve accuracy and mitigate ordering effects. The evaluation conditions were quiet standing to measure baseline metabolic rate, walking without the exoskeleton in the control boots ("No exoskeleton"), walking in the exoskeleton without assistance torques applied ("Unassisted"), and walking in the exoskeleton with torques applied ("Assisted").

Conditions were applied for different durations based on the novelty of the condition, where more novel walking conditions were longer to allow for user adaptation. Quiet standing and walking without the exoskeleton were six minutes long, with data analyzed over the last 3 minutes of each trial and averaged. Walking in the exoskeleton with no torques was measured over 10 minutes of walking, with data analyzed over the last 5 minutes of each trial and averaged. Walking with torques was measured over 20 minutes of

walking, with data analyzed over the last 5 minutes of each trial and averaged.

D. Optimization Protocol

Prior to the simulation study, the same user participated in an ongoing human-in-the-loop optimization experiment. The user participated in 5 days of human-in-the-loop optimization with hip-knee-ankle assistance using methods similar to [2]. This optimized assistance was evaluated similarly to the simulation-designed assistance for comparison.

E. Measurements

For each trial, metabolic rate was calculated from indirect calorimetry [17]. Oxygen consumption and carbon dioxide production were measured using a stationary metabolic cart (Cosmed Quark CPET). The participant fasted for 4 hours prior to metabolic measurements.

During the evaluation, muscle activity was measured using surface electromyography (EMG) with wireless electrodes (Delsys). Muscle activity was high-pass filtered with a cutoff frequency of 20 Hz, rectified, and then low-pass filtered with a cutoff frequency of 6 Hz [18], [19]. This measured activity was then averaged over all strides during the last 3 minutes of each trial as a function of percent stride. For each muscle, baseline activity was removed by subtracting the minimum value of the average profile for each condition. Activity was then normalized to the maximum of the unassisted condition for that muscle. Electrodes were placed based on a previous experimental protocol for recording EMG measurements in gait [20]. No uniarticular hip flexors were measured, but proximal rectus femoris activity was measured to capture activity related to hip flexion.

Vertical ground reaction forces were measured using an instrumented treadmill (Bertec) to allow for calculation of stride frequency. The applied torque and exoskeleton joint angles were also recorded using load cells, strain gauges and absolute magnetic encoders on the exoskeleton.

To evaluate the assumptions made by our simulation, we compared measured values for metabolics, kinematics, and stride frequency to the values expected from simulation. We focused on the simulation's ability to predict changes between the assisted and unassisted conditions, but also examined the absolute value of the estimated metrics.

IV. Simulation Results

The simulation-designed assistance strategy included device torques similar in shape to the hip and ankle plantarflexion experimental net joint moments, whereas the peak knee device torque was different from the knee joint moment (Fig. 2). The estimated metabolic cost of walking with assistance was 0.61 ± 0.20 W/kg across subjects, resulting in a 69.0% reduction in the metabolic cost of walking (Fig. 3A). The assistance nearly eliminated muscle activity produced by soleus and biceps femoris short head (Fig. 4). Activity in the iliopsoas, gastrocnemius, and gluteus maximus was reduced but not eliminated. The rectus femoris, semimembranosus, and vastus intermedius saw little to no reduction in muscle activity.

V. Experimental Results

A. Applied Torques

The exoskeleton was able to apply the torque profile designed in simulation with an RMS error of 0.013 N·m/kg at the hips, 0.043 N·m/kg at the knees, and 0.012 N·m/kg at the ankles (Fig. 2).

B. Metabolic Cost

The absolute metabolic cost of walking predicted by the simulation was less than what was measured in our experiment (Fig. 3). The baseline metabolic rate measured while standing was 1.37 W/kg. This baseline rate was excluded from all following measurements to measure specifically the cost of walking. The measured metabolic cost for walking without the exoskeleton ("Experimental, No exoskeleton") was 2.78 W/kg, which is similar to previously reported values for walking [21]. The unassisted simulation, which did not include exoskeleton masses, predicted a lower metabolic cost for walking of 1.96 W/kg ("Simulation, Unassisted"), but this difference in cost may be due to the lack of muscle groups that produce frontal plane motions, specifically the hip adductors-abductors.

The measured metabolic cost of walking with the simulation-designed torque profile ("Experimental, Assisted") was 2.68 W/kg. This is a reduction of 25.9% relative to walking in the device with no torque applied, which had a measured metabolic cost of 3.62 W/kg (Fig. 3, "Experimental, Unassisted"). This 25.9% reduction in the experiment is less than the 69.0% predicted by the simulation. The simulation thus accurately predicted that assistance could be provided that would reduce the cost of walking; however, the size of the reduction was substantially overestimated. Human-in-the-loop optimization of assistance with the same system resulted in a metabolic cost of walking of 1.75 W/kg ("Experimental, Assisted (HILO)"), corresponding to a 51.5% reduction relative to walking in the device unassisted. This reduction is about twice as large as the value achieved with the simulation-based torque profile, demonstrating that larger improvements are possible.

C. Muscle Activity

Fig. 4 shows the changes in muscle activity with assistance for 9 muscles for which EMG measurements were made along with the corresponding changes in the simulation. With exoskeleton assistance, measured muscle activity in the gastrocnemius and vastus lateralis decreased nearly to baseline. There were smaller reductions in activity in the soleus during stance and in the semitendinosus and biceps femoris near heel strike. Distal rectus femoris activity increased, while proximal activity increased and shifted in time. Tibialis anterior activity went mostly unchanged, with a small increase in activity in early swing. Activity in the gluteus maximus was unchanged.

While the simulation captured the direction of the changes in muscle activity, it did not accurately estimate the magnitude of change for many muscles. Simulation underestimated the magnitude of change for the gastrocnemius and vastus

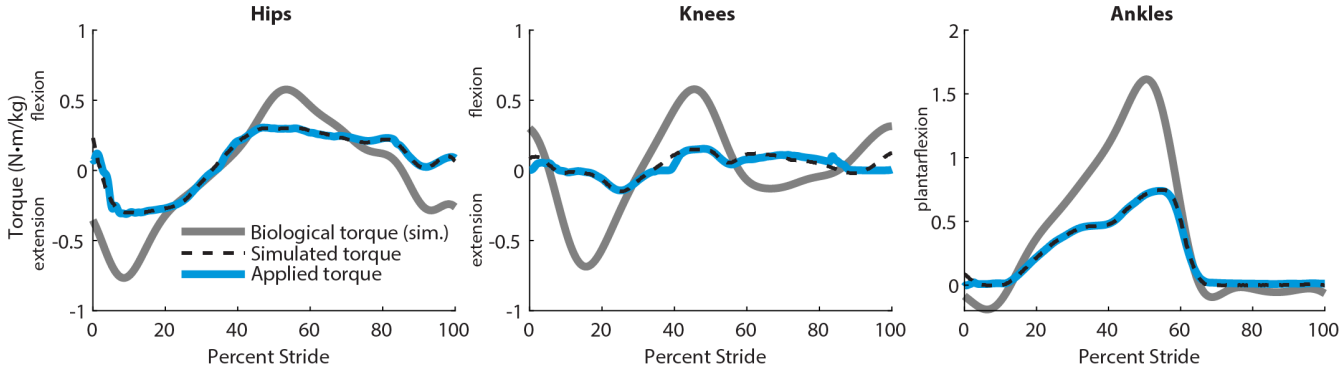

Fig. 2. **Biological, simulated, and applied torques.** The biological joint torques (gray) used in simulation were computed from subject data different from our experiment participant. The exoskeleton assistance strategy designed in simulation (black, dashed) was the desired torque profile during the experiment. Slight deviations between the desired torque and the torque actually applied using the exoskeleton in the experiment (blue) indicate torque-tracking errors. Applied torques were measured from the exoskeleton, averaged across both joints, and averaged as a function of percent stride.

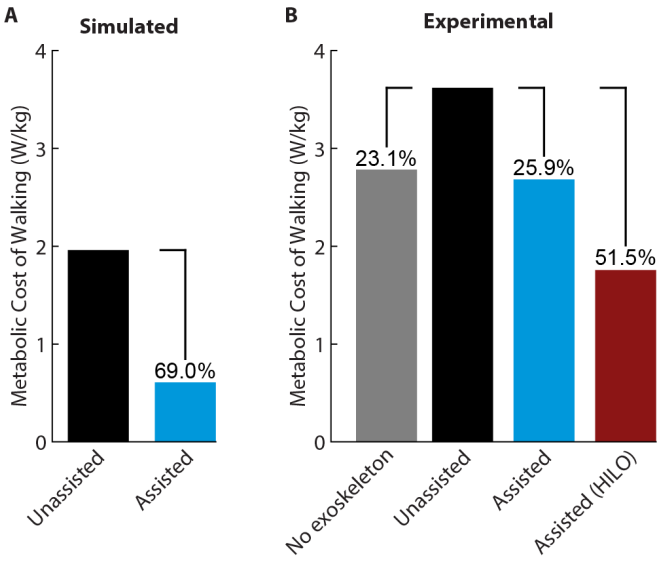

Fig. 3. **Metabolic cost of unassisted and assisted walking.** (**A**) The metabolic cost of walking predicted in simulation was computed without a baseline metabolic rate. Metabolic cost was predicted for the unassisted condition ("Unassisted", black) and with the simulated exoskeleton assistance ("Assisted", blue). (**B**) The baseline metabolic cost from quiet standing was subtracted from experimental metabolic cost measurements to evaluate the cost of walking. Metabolic cost was measured during walking without the exoskeleton ("No exoskeleton", gray), walking in the exoskeleton without applied torque ("Unassisted", black), and walking with torques designed in simulation ("Assisted", blue). The cost of walking in human-in-the-loop optimized assistance was measured on a separate day ("Assisted (HILO)", red). For both the simulation and experimental results, the values on top of each bar represent the percent reduction in metabolic cost relative to the unassisted condition.

lateralis. For the soleus, biceps femoris, and rectus femoris, the simulation overestimated the magnitude of the reduction. The overestimation in muscle activity changes could be related to simulations only minimizing metabolic cost or not considering kinematic adaptations, or missing modeling components that consider the effects of balance and comfort when walking. The overestimation of metabolic reductions may be related to this overestimation of reductions in muscle activity.

D. Kinematics

Exoskeleton joint kinematics measured at the hips and knees when walking in the unassisted condition were consistent with the kinematics used for the simulation, while the ankle plantarflexion angle in the simulation was increased throughout the gait cycle compared to the experimental unassisted condition (Fig. 5).

There were differences in kinematics between the experimental unassisted and applied-torque conditions. The average peak hip flexion angle increased by 9.8 degrees when torques were applied. Average peak hip extension angle decreased by 10.0 degrees with torque assistance. Peak knee flexion increased by 3.9 degrees, while peak knee extension decreased by 0.5 degrees, which is less than one standard deviation in measured angle over a walking trial. Peak plantarflexion angle increased by 15.9 degrees, while peak dorsiflexion angle also increased by 7.5 degrees. These experimental kinematic adaptations suggest that our inverse dynamics simulation approach was not sufficient to capture all true kinematic responses to assistance.

E. Stride Frequency

When walking without the exoskeleton, stride frequency was 0.810 $\pm$ 0.015 Hz. When walking in the exoskeleton without torque, stride frequency was slightly lower, with a mean of 0.804 $\pm$ 0.011 Hz. Stride frequency decreased when torques were applied, with a resulting stride frequency of 0.693 $\pm$ 0.013 Hz (13.8% decrease).

VI. Discussion

We successfully applied a torque profile designed in simulation and reduced the metabolic cost of walking. However, the simulation predicted a reduction in metabolic cost that was substantially larger than the reduction that was observed experimentally. The simulation assumed fixed segment movements and fixed net joint moments, but in the experiment we measured substantial changes in these outcomes. This suggests that kinematic and kinetic adaptations to assistance should be considered in future simulation-based optimizations.

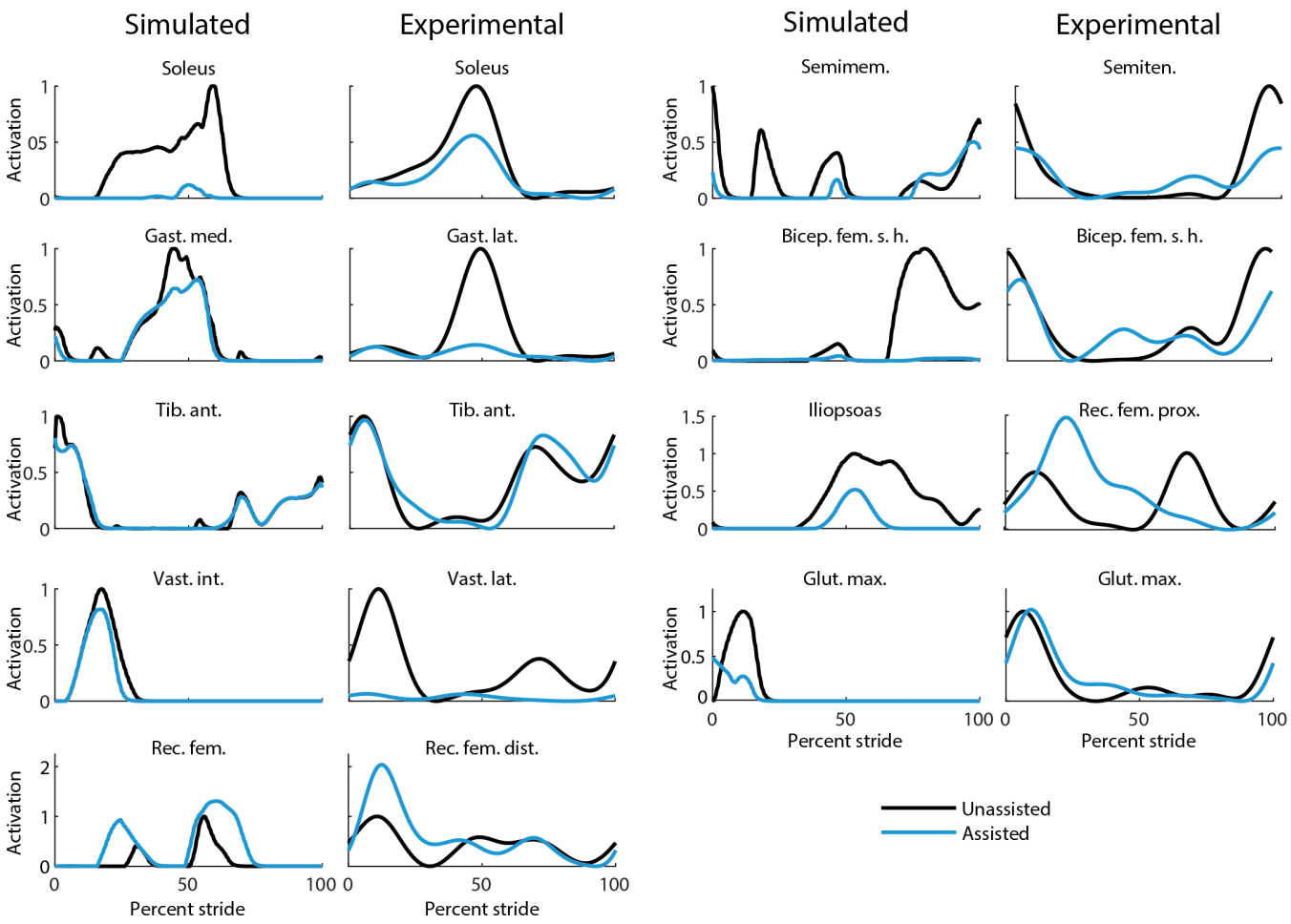

Fig. 4. **Simulated and measured muscle activity.** Muscle activity generated in simulation (first and third columns) is shown for the unassisted (black) and assisted (blue) conditions. For each muscle, activity was normalized to the peak activity of the unassisted condition. Muscle activity measured experimentally using electromyography (second and fourth columns) is shown for the unassisted (black) and assisted (blue) conditions. For each experimental condition, we subtracted the minimum value of the measured profile from the signal to remove baseline noise. Each simulated muscle was paired with the measured muscle that most closely represents its function.

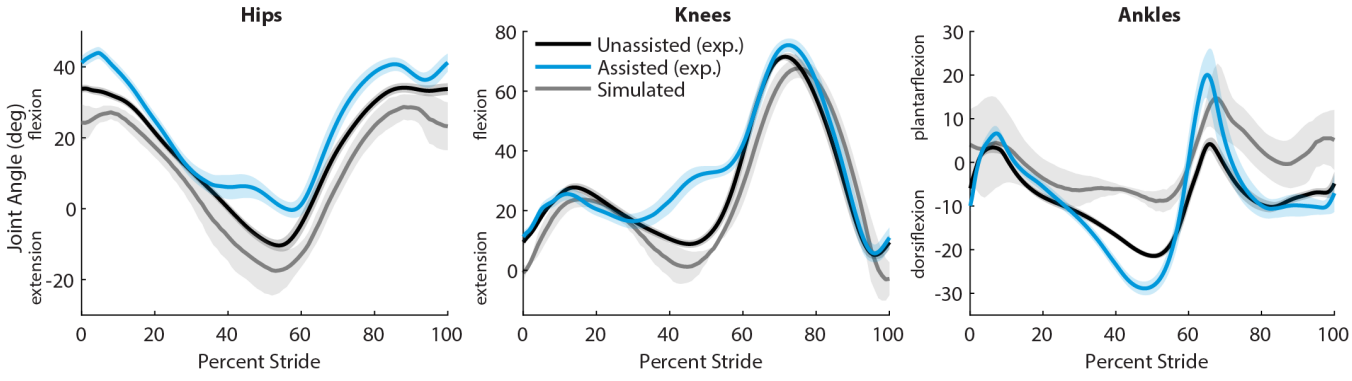

Fig. 5. **Simulated and measured kinematics.** Previously-collected biological joint angles (gray) from normal walking were used in simulation. Exoskeleton joint angles were measured during walking in the exoskeleton without torque (black) and with assistance torques applied (blue).

Only one experienced user participated in the experiment, and results could differ across users. We performed tests with an experienced user because we expected their expertise would enable them to quickly take advantage of exoskeleton assistance in general. We included a training protocol because we expected training to result in better performance with the simulation-based profile in particular. With an experienced, trained user, the assistance profile designed in simulation had the best chance at maximally reducing metabolic cost. However, it is possible that a different participant or further exposure could have led to a larger improvement in energy economy with simulation-designed assistance.

Simulation results in pilot testing produced torques greater than what could be safely applied in the experiment. Torque limits were necessary in subsequent simulations to find testable assistance strategies. Exoskeleton designers should consider that previous simulated assistance studies that do not impose empirical torque limits while designing new assistance strategies may overestimate the level of torque that can reasonably be applied to a user. This study suggests that predictive simulation methods are improved when including known torque limits, but future simulations should try to identify the factors underlying these limits so as to not require experimentally-identified values as inputs. Identifying these factors would make simulation tools more useful for exoskeleton design purposes.

Limitations in our simulation approach may have contributed to the differences between predicted and measured metabolic cost and muscle activity. Our chosen cost function may not have accurately reflected what our participant was trying to optimize while walking with assistance. The simulation cost function included a metabolic cost model, muscle activation, and tendon force rate, but did not consider user comfort when walking with large exoskeleton torques. The user was able to walk in the simulation-designed assistance strategy, but found it less comfortable than a profile designed using human-in-the-loop optimization, even though the two profiles had similar torque magnitudes. Another limitation was that our simulation was confined to the sagittal plane, which excluded muscle contributions to frontal and coronal plane motions. If we had included those muscles, such as the hip adductors and abductors, the overall energy cost of walking would be higher in both conditions, thereby reducing the percent change in energy cost with assistance. Similarly, we did not model exoskeleton mass or stiffness, and including these could increase absolute energy cost across conditions and reduce percent changes predicted. Finally, differences between the user's baseline kinematics and the kinematics used in the simulation may have produced a less effective assistance profile, limiting metabolic cost reductions. Future simulation work should use 3-D musculoskeletal models, allow predictions of kinematic adaptations, model exoskeleton mass and stiffness, and incorporate aspects of assistance that influence user comfort, such as costs for joint loading and eccentric muscle contractions.

Fully-predictive musculoskeletal simulations would be a groundbreaking accomplishment not only for exoskeleton device design but for the broader understanding of the biomechanics and neural control of gait. This study indicates an important step in the process: to experimentally validate simulation results. We show that experimental adaptation to exoskeleton assistance can differ from current simulation predictions. The findings here will help inform future simulation-based exoskeleton design to improve overall predictive accuracy. The identified limitations suggest that future simulations should consider 3-D kinematic adaptations to assistance, better validate metabolic models for whole-body energy changes, and update optimizer cost functions to better approximate how users adapt to assistance. These improvements to simulations will bring designers closer to rapid development of wearable robots and assistance strategies that improve human mobility.

ACKNOWLEDGMENT

We would like to thank K. Gregorczyk, G. Kanagaki, M. O'Donovan and the NSRDEC for their input on the exoskeleton system design and characteristics. P.W.F., G.M.B. and S.H.C. received funding from the U.S. Army Natick Soldier Research, Development and Engineering Center (W911QY18C0140). N.A.B. received funding from the National Science Foundation Graduate Research Fellowship Program and the Stanford Graduate Fellowship Program. J.L.H. and S.L.D. received funding from the National Institutes of Health (P2C HD065690).

REFERENCES

[1] A. J. Young and D. P. Ferris, "State of the art and future directions for lower limb robotic exoskeletons," *IEEE Trans. Neural. Syst. Rehabil. Eng.*, vol. 25, pp. 171-182, 2017.

[2] J. Zhang, P. Fiers, K. A. Witte, R. W. Jackson, K. L. Poggensee, C. G. Atkeson, and S. H. Collins, "Human-in-the-loop optimization of exoskeleton assistance during walking," *Science*, vol. 356, pp. 1280–1284, 2017.

[3] Y. Ding, M. Kim, S. Kuindersma, and C. J. Walsh, "Human-in-the-loop optimization of hip assistance with a soft exosuit during walking," *Sci. Robot.*, vol. 3, eaar5438, 2018.

[4] T. K. Uchida, A. Seth, S. Pouya, S., C. L. Dembia, J. L. Hicks, and S. L. Delp, "Simulating ideal assistive devices to reduce the metabolic cost of running," *PLoS ONE*, vol. 11, e0163417, 2016.

[5] C. L. Dembia, A. Silder, T. K. Uchida, J. L. Hicks, and S. L. Delp, "Simulating ideal assistive devices to reduce the metabolic cost of walking with heavy loads," *PLoS ONE*, vol. 12, e0180320, 2017.

[6] E. P. Grabke, K. Masani, and J. Andrysek, "Lower Limb Assistive Device Design Optimization Using Musculoskeletal Modeling: A Review," *Journal of Medical Devices*, vol. 13(4), https://doi.org/10.1115/1.4044739, 2019.

[7] G. Lee, J. Kim, F. A. Panizzolo, Y. M. Zhou, L. M. Baker, I. Galiana, P. Malcolm, and C. J. Walsh, "Reducing the metabolic cost of running with a tethered soft exosuit," *Sci. Robot.*, vol. 4, eaan6708, 2017.

[8] C. F. Ong, T. Geijtenbeek, J. L. Hicks, and S. L. Delp, "Predicting gait adaptations due to ankle plantarflexor muscle weakness and contracture using physics-based musculoskeletal simulations," *PLOS Comp. Bio.*, vol. 15(10), e1006993, 2019.

[9] E. M. Arnold, S. R. Hamner, A. Seth, M. Millard, and S. Delp, "How muscle fiber lengths and velocities affect muscle force generation as humans walk and run at different speeds," *Journal of Experimental Biology*, vol. 216(11), pp. 2150-2160, 2013.

[10] A. Seth, J. L. Hicks, T. K. Uchida, A. Habib, C. L. Dembia, et al., "OpenSim: Simulating musculoskeletal dynamics and neuromuscular control to study human and animal movement," *PLOS Comp. Bio.*, vol. 14(7), e1006223, 2018.

[11] G. G. Handsfield, C. H. Meyer, J. M. Hart, M. F. Abel, and S. S. Blemker, "Relationships of 35 lower limb muscles to height and body mass quantified using MRI," *J. Biomech.*, vol 47., pp. 631-638, 2014.
[12] A. Silder, B. Whittington, B. Heiderscheit, and D. G. Thelen, "Identification of passive elastic joint moment-angle relationships in the lower extremity," *J. Biomech.*, vol. 40, pp. 2628-2635, 2007.
[13] F. De Groote, A. L. Kinney, A. V. Rao, and B. J. Fregly, "Evaluation of Direct Collocation Optimal Control Problem Formulations for Solving the Muscle Redundancy Problem," *Ann. Biomech. Eng.*, DOI: 10.1007/s10439-016-1591-9, 2016.
[14] B. R. Umberger, K. G. M. Gerritsen, P. E. Martin, "A Model of Human Muscle Energy Expenditure," *Comput. Method Biomec.*, vol. 6, pp. 99-111, 2003.
[15] A. D. Koelewijn, E Dorschky, and A. J. van den Bogert, "A metabolic energy expenditure model with a continuous first derivative and its application to predictive simulations of gait," *Comput. Methods Biomech. Biomed. Engin.*, vol. 21, pp. 521-531, 2018.
[16] G. M. Bryan, P. W. Franks, S. C. Klein, R. J. Peuchen, S. H. Collins, "A hip-knee-ankle exoskeleton emulator for studying gait assistance," *in review*.
[17] J. M. Brockway, "Derivation of formulae used to calculate energy expenditure in man," *Hum. Nutr. Clin. Nutr.*, vol. 41C, pp. 463–471, 1987.
[18] C. J. De Luca, L. D. Gilmore, M. Kuznetsov, and S. H. Roy, "Filtering the surface emg signal: Movement artifact and baseline noise contamination," J. Biomech., vol. 43, pp. 1573–1579, 2010.
[19] R. W. Jackson and S. H. Collins, "Heuristic-based ankle exoskeleton control for co-adaptive assistance of human locomotion," *IEEE T. Neur. Sys. Reh.*, vol. 27, no. 10, pp. 2059-2069, 2019.
[20] D. A. Winter and H. J. Yack, "EMG profiles during normal human walking: stride-to-stride and inter-subject variability," *Electroencephalogr. Clin. Neurophysiol.*, vol. 67, pp. 402-411, 1987.
[21] R. L. Waters, S. Mulroy, "The energy expenditure of normal and pathologic gait," *Gait & Posture*, vol. 9, pp. 207-231, 1999.